

## POLYHARMONIC METAL DETECTOR

Jakub Svatos<sup>1,2</sup>, Miloslav Linda<sup>1</sup>

<sup>1</sup>Czech University of Life Sciences Prague; <sup>2</sup>Czech Technical University in Prague  
jsvatos@tf.czu.cz, linda@tf.czu.cz

**Abstract.** The article deals with usage of polyharmonic signals to metal detection and discrimination. A substantial problem of all conventional eddy current metal detectors (induction devices in general) is in limited possibilities of identification of detected objects. The excitation signal and signal processing in the detector should be done in a way to better characterize the detected object. Usage of the polyharmonic excitation signal and processing of the signal brings an opportunity to improve the detection ability. A suitable polyharmonic excitation signal is  $\sin(x)/x$  – sinc signal. Experimental measurements were processed in frequency domain using Discrete Fourier Transformation. Amplitude and phase spectra together with polar graphs are presented. As experimental targets different ferromagnetic and non-ferromagnetic materials were used.

**Keywords:** metal detection, eddy currents, polyharmonic signal, sinc, identification.

### Introduction

Metal detection is an important part of our lives from the beginning of the 20<sup>th</sup> century to present time. There are many methods to detect metal objects or mine [1] but eddy current metal detectors are still the most popular detectors. Eddy current metal detectors are used not only in military but are also widely used in pharmacy, food, beverage, chemical industries or in agriculture. The biggest disadvantage of eddy current metal detectors is in identifying of the detected object [2]. The excitation signal and signal processing in the detector should be done in a way to better characterise the detected object. Use of multi-tone excitation signals can be considered. Such signals should be composed of suitable frequencies and the resulting received signal spectrum can be evaluated.

As a suitable signal  $\sin(x)/x$  can be considered. Using of  $\sin(x)/x$  brings to an opportunity to evaluate the received signal in the whole frequency spectrum. Such an excitation signal can be defined and programmed in mathematical software for example in Scilab or MATLAB and can be generated by a common arbitrary generator which can generate very low frequencies (ca. 1-50 kHz).

The application of polyharmonic excitation signals brings an opportunity for better response in a wide range of frequencies, and therefore more extensive and complex set of data for the signal analysis is available. Thanks to the multi-frequency approach, the wide band of the Response function of the detected object is covered [3]. More details about the Response function can be found in [4] or [5].

Analysis of ferromagnetic and non-ferromagnetic materials is used in sectors where separation of feedstock is necessary, such as waste, for example. Thanks to the described method detection of a wide range of ferrous and non-ferrous materials such as bronze, brass and various irons, which are commonly used, can be done. The system can be implemented, for example, as walkthrough box systems with coils.

### Materials and methods

All measurements were taken on the search head of the metal detector ATMID [6]. The ATMID search head uses a Double-D coil configuration with a diameter of 260 mm. The electrical equivalent circuit diagram of the Double-D search head of ATMID metal detector is presented in Fig. 1.

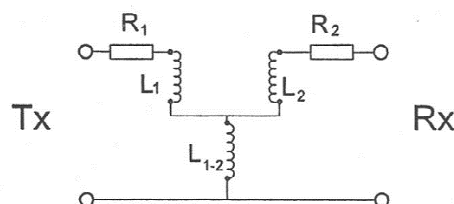


Fig. 1. Equivalent circuit diagram of the ATMID coil

$R_1$  is ohmic resistance and  $L_1$  is inductance of the transmitting coil (TX),  $R_2$  is ohmic resistance,  $L_2$  is inductance of the receiving coil (RX) and  $L_{1-2}$  corresponds to the mutual inductance between the coils. T-shape configuration of inductances in Fig. 1 corresponds to the transformer with inductances  $L_1$  of primary and  $L_2$  of secondary winding and mutual inductance  $M$  between both windings. The measured parameters for operating frequency of 8.17 kHz are listed in Table 1. The number of turns of the transmitting coil is 17 and the receiving coil – approx. 190 turns.

Table 1

**Electromagnetic properties of materials**

$R_1$ ( $\Omega$ )	$L_1$ (mH)	$R_2$ ( $\Omega$ )	$L_2$ (mH)	$M$ ( $\mu$ H)
1.2	0.774	182	3.35	0.1

The frequency range of all measurements was below the resonant frequency of the coils (transmitting coil about 90 kHz, receiving coil about 45 kHz).

Homogenous spheres of different sizes from non-ferromagnetic or ferromagnetic materials were used as test targets. The measured materials and their electromagnetic properties are presented in Table 2.

Table 2

**Electromagnetic properties of materials**

Material	Conductivity $\sigma$ ( $S \cdot m^{-1}$ )	Relative permeability $\mu_r$	Skin depth $\delta$ (mm) at $f = 1$ kHz	Skin depth $\delta$ (mm) at $f = 25$ kHz
Brass	1.500	1	4.11	0.82
Bronze	0.740	1	5.85	1.17
INOX AISI 420	0.139	600	0.55	0.11
AISI 100Cr6	0.465	300	0.43	0.08

The sine cardinal signal or commonly referred function sinc is one of the polyharmonic signals which can be suitable for metal detector excitation to cover a wide range of the response of the detected object. The spectrum of the sinc function is appropriate for further spectral analysis. The number and position of the spectral lines could be easily set and defined [7]. Another advantage is that all frequencies are applied at once.

A modified sinc signal, which is used for the next experiments, is composed of two sinc signals with the same parameters, where the second half of the period is inverted (Fig. 2).

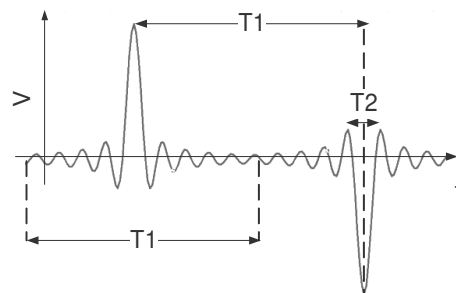


**Fig. 2. Time plot of excitation modified sinc signal**

One period of the signal is described by the formula:

$$u(t) = H\left(t + \frac{T_1}{2}\right) \left[ \frac{\sin\left(\frac{2\pi}{T_2}\right)}{\frac{2\pi}{T_2}} \right] - H\left(t - \frac{T_1}{2}\right) \left[ \frac{\sin\left(\frac{2\pi}{T_2}\right)}{\frac{2\pi}{T_2}} \right], \tag{1}$$

where  $H$  – Heaviside function,  
 $t$  – time, seconds;

$T_1$  – period of the lowest frequency, seconds;

$T_2$  – period of the highest frequency, seconds.

The Heaviside function chops the segment of the sinc function in the time range  $< -T_{1/2}, T_{1/2}$ ). The anti-symmetrical signal covers full scale of the digitizer and allows to continuous crossing between the periods.

Spectrum has a rectangular shape with equidistantly distributed frequencies. The number of spectral lines is given by ratio of the  $T_1$  and  $T_2$ . The first spectral line is at frequency  $f_1 = 1/T_1$  and the last is at  $f_2 = 1/T_2$ . The spectrum of its derivative has an ascending shape which follows the derivative of the function, but the character of the spectrum is unchanged. It has been advantageous to use integral of sinc function. Antiderivative of sinc function is *Sine Integral* function  $\text{Si}(x)$ . Since the definition and generation of  $\text{Si}(x)$  are not simple, a modified sinc function has been used.

Since the coil is excited by current  $i_L$ , its voltage  $u_L$  corresponds to the first derivative (2).

$$u_L = L \frac{di_L}{dt}, \quad (2)$$

where  $u_L$  – voltage, volts;

$L$  – inductance, henry;

$i_L$  – current, ampere;

$t$  – time, seconds.

First derivative of the sinc signal is defined:

$$\frac{d}{dt} \text{sinc}(\pi t) = \frac{\pi t \cdot \cos(\pi t) - \sin(\pi t)}{(\pi)^2}. \quad (3)$$

The measurement setup consisted of a 14-bit programmable function generator AFG 3102 and Teledyne LeCroy HDO6104 High Definition Oscilloscope (15-bit digitizer) connected to PC. The generator used external synchronization from the oscilloscope. The block diagram of the measurement setup is in Fig. 3.

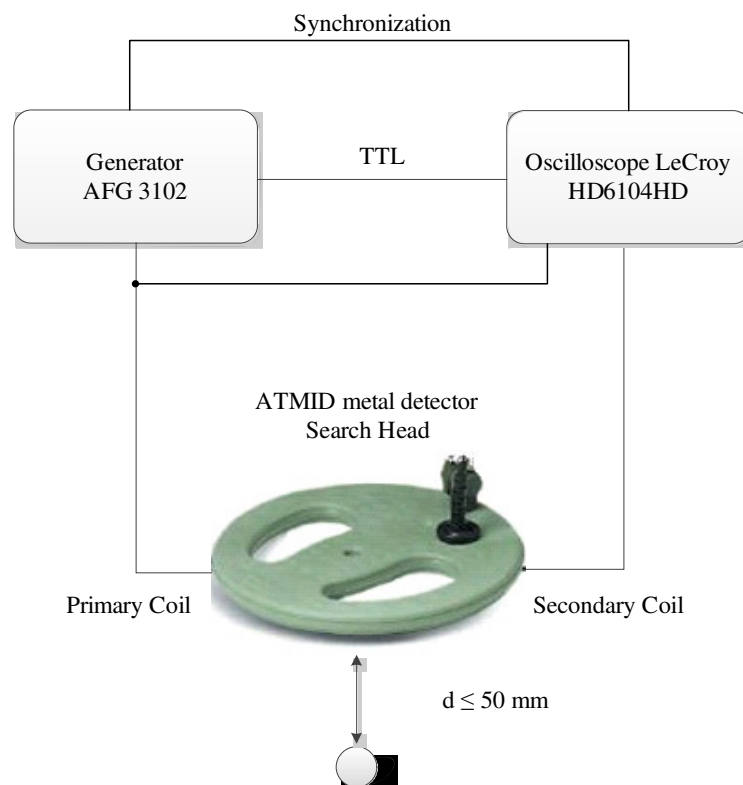


Fig. 3. Block diagram of the measurement setup

## Results and discussion

The targets were placed and measured in open air. The excitation signal was driven through the transmitting coil of ATMID metal detector. The measured data were mostly processed in MATLAB. The following parameters describe the used modified sinc signal, the frequency  $f_1 = 1/T_1 = 0.5$  kHz,  $f_2 = 1/T_2 = 10$  kHz, 10 significant carrier frequencies, and amplitude of 10 V. From these parameters repeating frequency of  $f_R = 1$  kHz follows and significant frequencies at each 2 kHz.

Firstly, the signal was filtered by the Finite Impulse Response (FIR) band-pass filter of 300<sup>th</sup> order. Lower frequency of the band pass filter was  $f_d = 1$  kHz and upper frequency  $f_h = 30$  kHz. These filtered signals were after processed by Discrete Fourier Transform (DFT) using a Fast Fourier Transform (FFT) algorithm, and were computed from the number of samples  $N = 1048578$ , which is the nearest powers of two from 1 MSamples. The phase spectra were calculated from a complex variable definition. All presented phase spectra were computed as a difference between the phase spectrum of the signal which corresponds to measurement without any target (background, no object) and the phase spectrum of the signal which corresponds to measurement with a testing target. For better presentation and comparison, the spectra of comparing signals which are presented are shifted by  $\pm 100$  Hz. This is done for better presentation only.

Fig. 4 shows the measured amplitude and phase spectra corresponding to ferromagnetic steels AISI 52100 100Cr6 and INOX AISI 420 for two different sphere diameters (10 mm and 20 mm). In the case of the multiple carriers, the frequency characteristic of the measured object covers a wide range of Response Function. Amplitude spectra which correspond to these materials are greater at all frequencies than the amplitude spectra of the signal which corresponds to no object present. This is caused by ferromagnetic material permeability which is much greater than one. In general, magnitude spectra are getting higher for all ferrous materials with increasing diameter of the sphere. Magnitudes on low frequencies increase more significantly than at higher frequencies, which can be caused by the character of the Response Function and goes to its inductive limit [3]. The phase shift difference shows that ferrous materials shift the phase from positive values to negative. For greater diameter, the absolute phase shift is increasing but the relative phase shift due to getting closer to the inductive limit is decreasing apparently. Amplitude spectra of both materials show noticeable increases at lower frequencies.

The difference between these two materials is in the trend of the amplitude and phase spectra. For better interpretation and differentiation X-Y chart is shown in Fig. 6 (left). The measurements also show that the distinction between different similar ferromagnetic objects cannot be done easily if only one frequency is used.

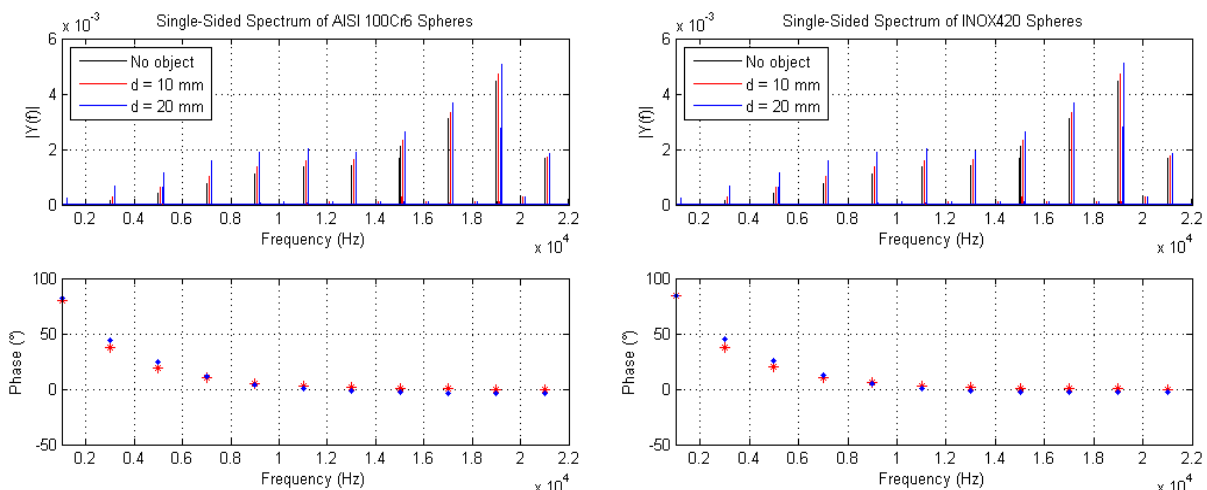


**Fig. 4. Amplitude spectra and phase spectra corresponding to AISI 52100 100Cr6 sphere (left) and INOX AISI 420 sphere (right) with diameters of 10 mm and 20 mm**

Fig. 5 shows the measured amplitude and phase spectra corresponding to non-ferromagnetic materials – brass and bronze for two different sphere diameters (10 mm and 20 mm). The amplitude spectra of non-ferrous materials shows essential difference from ferrous materials. At higher

frequencies the phase shift of the signal causes the suppression of the induced voltage. This causes drop of spectral lines at higher frequencies. The phase shift caused by non-ferromagnetic objects goes to negative values. At lower frequencies the phase difference between the signal which corresponds to non-ferrous materials and the signal which corresponds to the measurement without any target present is bigger as the diameter of the sphere is getting larger. At higher frequencies a similar situation as for ferromagnetic materials occurs; the relative phase shift decreases and the absolute phase shift gets bigger with larger diameter of spheres.

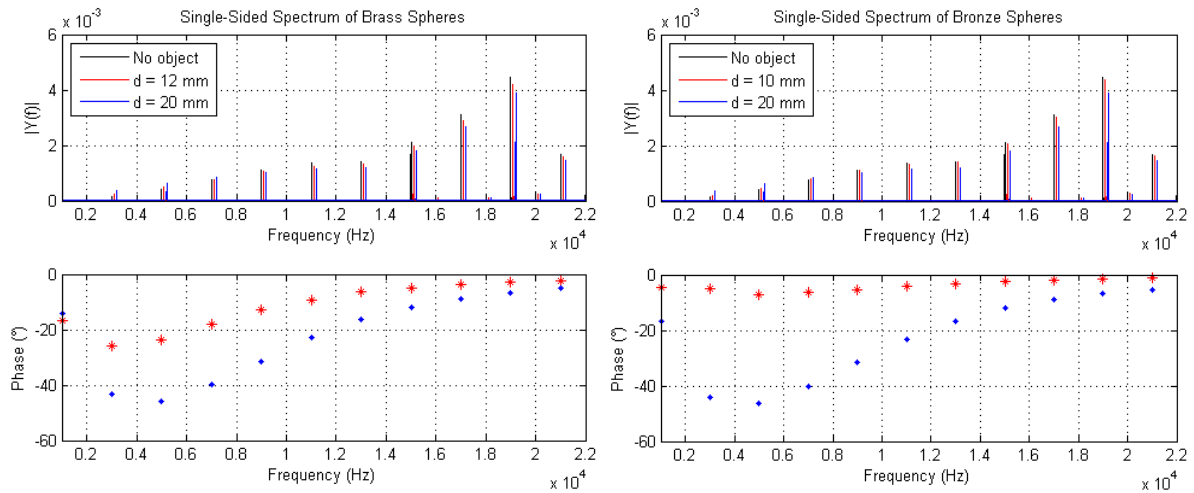


**Fig. 5. Amplitude spectra and phase spectra corresponding to brass sphere (left) and bronze sphere (right) with diameters of 10 mm, 12 mm and 20 mm**

Similarly the difference between the measured non-ferrous materials is in the trend of the amplitude and phase spectra. This difference between the measured ferrous and non-ferrous materials is apparent on the presented X-Y chart (Fig. 6).

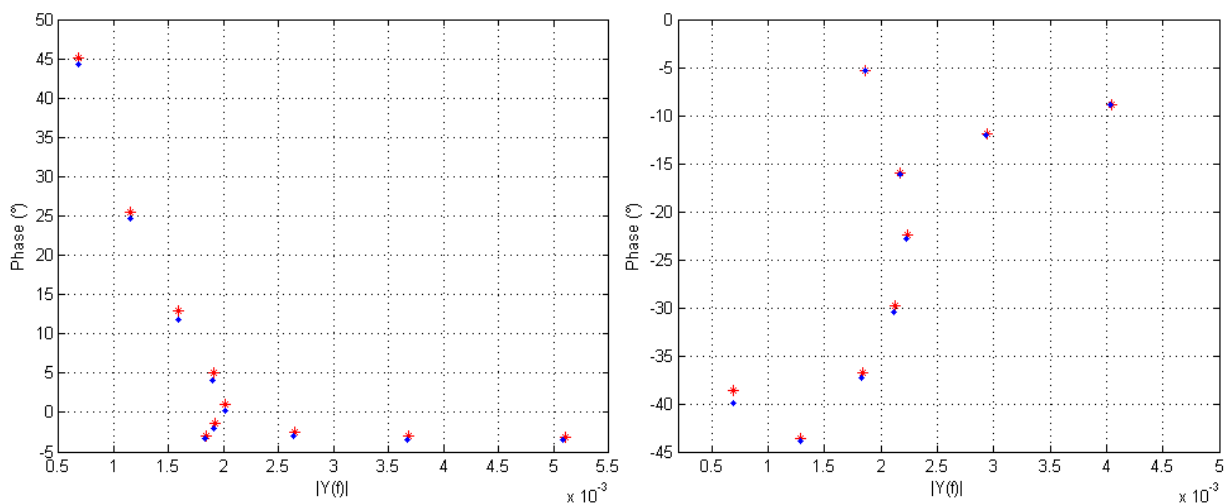


**Fig. 6. X-Y chart of amplitude and phase spectra corresponding to AISI 420 (red) and AISI 52100 100Cr6 (blue) sphere with diameters of 20 mm (left) and brass (red) and bronze (blue) material with diameter 20 mm (right)**

The phase difference corresponding to ferrous materials is slightly larger than 1 degree at lower frequencies and slightly smaller than 1 degree at higher frequencies; the difference between both materials is in the trend of the phase spectrum. The difference between the amplitude spectra is minimal. The biggest difference is at the 10th harmonic; at the highest frequency. Comparing non-ferromagnetic materials with similar electromagnetic properties (brass and bronze) a similar situation occurs. The difference in the amplitude spectrum increases with increasing the frequency. The phase

spectra difference decreases with increasing the frequency. The phase difference at lower frequencies is about 1.5 degree for lower frequencies and only about 0.2 degree for higher frequencies.

In general, the experiment shows that the phase difference between similar ferromagnetic or non-ferromagnetic materials decreases with the diameter. In addition, at higher frequencies the difference between the amplitude spectra of similar materials gets bigger in contrast to the phase spectra difference. The phase difference between similar materials gets smaller with increasing the frequency.

## Conclusions

Several experiments were done using  $\sin(x)/x$  signal on All Terrain Metal Detector. Evaluation of the received signal has been done in frequency domain. Signal processing by means of DFT using FFT algorithm were done. The processed data contain the amplitude and phase spectra. The Response function of the detected object over a wide band of frequencies.

Based on the experimental results, use of sinc excitation signals allows possible identification and discrimination of the detected objects. The application of polyharmonic excitation signals bring an opportunity for better response in a wide range of frequencies, and therefore a more extensive and complex set of data for the signal analysis is available. The experiments show that thanks to the multiple frequencies approach, differentiation between even similar objects (in a way of electromagnetic response) can be done.

## Acknowledgment

This research was supported by the Grants SGS14/153/OHK3/2T/13 “Systems of Data Processing and Fusion for Diagnostics and Measurement Applications” by the Grant Agency of the Czech Technical University in Prague.

## References

1. Bielecki Z., Janucki J., et al. Sensors and Systems for the Detection of Explosive Devices – An Overview. Metrology and Measurement Systems, vol. XIX, no. 1. 2012, pp. 3-28.
2. Composite Autors. Metal Detector Basics and Theory.Minelab. 2012. Available at: [http://www.minelab.com/\\_\\_files/f/11043/METAL%20DETECTOR%20BASICS%20AND%20THEORY.pdf](http://www.minelab.com/__files/f/11043/METAL%20DETECTOR%20BASICS%20AND%20THEORY.pdf)
3. Svatos J., Vedral J., Fexa P. Metal Detector Excited by Frequency Swept Signals. Metrology and Measurement Systems.vol. XVIII, no. 1, 2011, pp. 57-68.
4. Bruschini C.A Multidisciplinary Analysis of Frequency Domain Metal Detectors for Humanitarian Demining. Dissertation thesis, VrijeUniversiteitBrusse, 2002.
5. Riggs L.S., Mooney J.E., Identification of Metallic Mine-Like Objects Using Low Frequency Magnetic Fields. IEEE Transactions on Geoscience & Remote Sensing, vol. 39, no. 1, 2001.
6. Schiebel. ATMID Maintenance Manual MT5001/16/010E.
7. Olver F.W.J., Lozier D.M., Boisvert R.F., Clark, Charles W., et al. Numerical methods. NIST Handbook of Mathematical Functions, Cambridge University Press, 2010.